



**HAL**  
open science

# Storage management in a rolling horizon Dynamic Real-Time Optimization (DRTO) methodology for a non-concentrating solar thermal plant for low temperature heat production

Alix Untrau, Sabine Sochard, Frédéric Marias, Jean-Michel Reneaume, Galo A.C. Le Roux, Sylvain Serra

## ► To cite this version:

Alix Untrau, Sabine Sochard, Frédéric Marias, Jean-Michel Reneaume, Galo A.C. Le Roux, et al.. Storage management in a rolling horizon Dynamic Real-Time Optimization (DRTO) methodology for a non-concentrating solar thermal plant for low temperature heat production. Applied Energy, 2024, 360, pp.122860. 10.1016/j.apenergy.2024.122860 . hal-04507057

**HAL Id: hal-04507057**

**<https://univ-pau.hal.science/hal-04507057>**

Submitted on 15 Mar 2024

**HAL** is a multi-disciplinary open access archive for the deposit and dissemination of scientific research documents, whether they are published or not. The documents may come from teaching and research institutions in France or abroad, or from public or private research centers.

L'archive ouverte pluridisciplinaire **HAL**, est destinée au dépôt et à la diffusion de documents scientifiques de niveau recherche, publiés ou non, émanant des établissements d'enseignement et de recherche français ou étrangers, des laboratoires publics ou privés.

# Storage management in a rolling horizon Dynamic Real-Time Optimization (DRTO) methodology for a non-concentrating solar thermal plant for low temperature heat production

Alix Untrau<sup>a,\*</sup>, Sabine Sochard<sup>a</sup>, Frédéric Marias<sup>a</sup>, Jean-Michel Reneaume<sup>a</sup>,  
Galo A.C. Le Roux<sup>b</sup>, Sylvain Serra<sup>a</sup>

<sup>a</sup>*Université de Pau et des Pays de l'Adour, E2S UPPA, LaTEP, Pau, France*

<sup>b</sup>*Universidade de São Paulo, Escola Politécnica, São Paulo, Brasil*

---

## Abstract

The intermittency and uncertain forecasts of solar irradiation complicate the operation of a solar thermal plant with thermal storage for heat production. In this work, a rolling horizon Dynamic Real-Time Optimization (DRTO) methodology is proposed to determine the economic optimal operation of a non-concentrating solar thermal plant for low temperature heat production, using a planning phase to improve storage management. The methodology is tested online on a detailed simulation model representing a large-scale solar thermal plant in case studies, using variable heat demand and real data for the weather forecasts and measurements. It was shown that DRTO performs better than offline Dynamic Optimization thanks to the use of updated weather forecasts and the regular re-initialization of the system state using measurements. An increase up to 57% in supplied energy and a decrease up to 35% in operating costs were achieved with DRTO compared to DO. Guidelines on the best storage management policy at the DRTO level, using the planning phase, are formulated. While storing the maximum energy possible for later use is the best option when overheating is not a risk, following the planned storage state helps to prevent overheating when the solar irradiation is high and the heat demand low.

---

\*alix.untrau@univ-pau.fr

*Keywords:* Dynamic Real-Time Optimization, Solar Thermal Energy, Simulation, Storage management

---

## **Nomenclature**

### **Abbreviations**

CSP	Concentrated Solar Power
DAE	Differential Algebraic Equation
DHN	District Heating Network
DO	Dynamic Optimization
DRTO	Dynamic Real-Time Optimization
DRTO E	DRTO Economic
DRTO M	DRTO Maximum
DRTO P	DRTO Planning
GHI	Global Horizontal Irradiance [ $W.m^{-2}$ ]
MAPE	Mean Absolute Percentage Error
MPC	Model Predictive Control
NLP	Nonlinear Programming
NTU	Number of Transfer Units
OCFE	Orthogonal Collocation on Finite Elements
ODE	Ordinary Differential Equation
OF	Objective Function
OF <sub>eco</sub>	Economic Objective Function [€]

PDE	Partial Differential Equation
PID	Proportional Derivative Integral
RTO	Real-Time Optimization
TES	Thermal Energy Storage

### **Greek Symbols**

$\beta$	Scalar characterizing the steepness of the sigmoid function
$\Delta z$	Height of a discretization layer in the storage tank [ $m$ ]
$\delta$	Threshold for the sigmoid function
$\gamma_{var}$	Weight on the penalty term to smooth the flow rates trajectories
$\lambda$	Scalar used in a soft constraint
$\omega$	Weight on the storage state tracking term
$\Phi_{var}$	Penalty term to smooth the flow rates trajectories
$\rho$	Fluid density [ $kg.m^{-3}$ ]

### **Subscripts and superscripts**

amb	Ambient
cold	Cold side of a heat exchanger
consumer	Consumer stream
demand	Heat demand
elec	Electric
hot	Hot side of a heat exchanger
HX	Heat Exchanger

in	Inlet of the element
mean	Mean value
out	Outlet of the element
s	Storage
SF	Solar Field

### Latin Symbols

$\dot{m}$	Mass flow rate [ $kg.s^{-1}$ ]
$\dot{P}$	Power [ $W$ ]
$\dot{Q}$	Heat flow [ $W$ ]
$A$	Area [ $m^2$ ]
$C_p$	Fluid heat capacity [ $J.kg^{-1}.K^{-1}$ ]
$C_{tot}$	Total operating costs (electricity and gas) for a simulation [€]
$E$	Energy [ $MWh$ ]
$E_{stock\ final}$	Energy stored in the storage tank at the end of the simulation [ $MWh$ ]
$E_{stored}$	Energy stored in the storage tank [ $MWh$ ]
$E_{supplied}$	Energy supplied to the consumer [ $MWh$ ]
$ElecPrice$	Price of electricity [€/MWh]
$GasPrice$	Price of gas [€/MWh]
$HeatPrice$	Price of heat [€/MWh]
$k$	Fluid thermal conductivity [ $W.m^{-1}.K^{-1}$ ]
$M$	Fixed scalar used in inequalities representing discontinuities

$N$	Number of discretization layers in the storage tank
$P$	Perimeter [ $m$ ]
$R_{th}$	Thermal resistance [ $K.W^{-1}$ ]
$S_l$	Lateral surface of a tank layer [ $m^2$ ]
$T$	Temperature [ $^{\circ}C$ ]
$t$	Time [ $s$ ]
$U$	Overall heat transfer coefficient [ $W.m^{-2}.K^{-1}$ ]
$z$	Tank height from the bottom of the tank [ $m$ ]

## 1. Introduction

The energy transition is necessary to mitigate climate change and keep the global warming below  $2^{\circ}C$  as aimed by the Paris agreements [1]. Heat represents more than 50% of the final energy consumption in the world, and its production mostly relies on fossil fuels nowadays [2]. Therefore, increasing the part of renewable heat is crucial to achieve the energy transition objectives fixed worldwide and locally. For example, in Europe, the Revised Renewable Energy Directive [3] targets an increase of 1.3% per year in the share of renewable energy in the heating and cooling sectors for each state member. Solar thermal energy represents a good alternative to fossil fuels for the production of heat, especially at low temperatures. Indeed, it uses a renewable source of energy, the sun irradiation, to produce heat without direct  $CO_2$  emissions [4].

### 1.1. Solar thermal plant potential and challenges

In this work, non-concentrating solar thermal plants are considered, which are used for low temperature heat production ( $< 100^{\circ}C$  [5]). The heat can be supplied to district heating networks for domestic use or to industries requiring low temperature heat such as the food and beverage industries [6]. The use of

the existing solar thermal systems for heat production in 2020 led to savings of 43.8 million tons of oil corresponding to 141.3 million tons of CO<sub>2</sub> emissions, according to the annual report from the International Energy Agency [7]. This shows that using solar thermal energy instead of fossil fuels for heat production is a promising alternative to achieve the necessary energy transition. The challenge with solar thermal energy is its intermittency, with daily and seasonal variations, that are difficult to predict accurately. Moreover, the heat demand is also variable in most cases. In order to decouple the solar heat production from the heat consumption, Thermal Energy Storage (TES) is used. In a low temperature solar thermal plant, the most common daily storage technology is the stratified water tank, because of its low cost and simplicity [4], and was chosen in this study. The association of the solar field and the TES makes the operation of the solar thermal plant complex. Indeed, there are different operational modes: direct supply of the solar heat, charge or discharge of the storage tank or shut down of heat supply if there is no solar heat available. Optimization methodologies appear particularly promising for the operation of solar thermal plants because of their various degrees of freedom.

### *1.2. State of the art on solar thermal plant optimal operation*

The design of a solar thermal plant, such as the solar collectors total area and storage tank capacity, can be optimized to minimize the investment cost while satisfying the heat demand when using standard operating strategies. For example, the design of a solar thermal plant supplying heat to a District Heating Network (DHN) has been optimized in ([8], [9] and [10]), while similar work was conducted in ([11] and [12]) with solar heat for industrial processes. For a correctly designed system, the optimization of the operation can also improve performances of the solar thermal plant. For example, Krause *et al.* showed a reduction of 0.6% in the cost of solar heat thanks to dynamic optimization of the operation of a well-designed system [13]. Although the improvement seems small, given the large cost of a solar thermal plant, it can still lead to important savings, making solar heat more competitive against fossil fuels [14].

The optimization of the transient operation of a solar thermal plant is the focus of the present paper.

The operation of a system can be decomposed into several hierarchical layers, as shown in Figure 1.

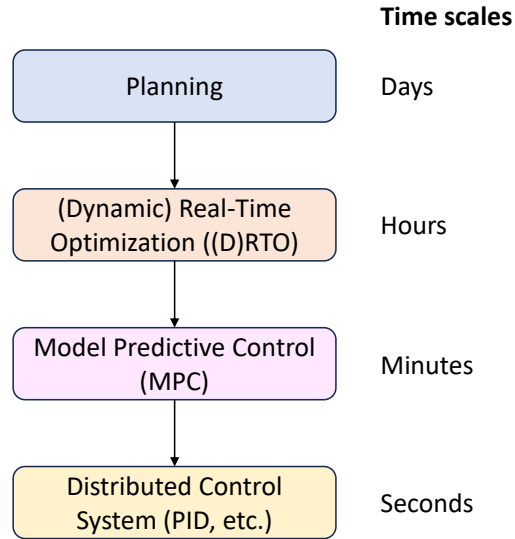


Figure 1: Hierarchical structure of control and decision making in a plant(adapted from [15])

The bottom layer corresponds to the distributed regulatory control. It is always present in a solar thermal plant and is usually the only layer used, with the operation determined by logic rules which are tracked by basic controllers such as Proportional Integral Derivative (PID) [14]. Nevertheless, a solar thermal plant is a complex system, showing highly nonlinear behavior, undergoing variable energy source and demand, and composed of elements with various dynamics. Thus, advanced multivariable controllers, such as Model Predictive Control (MPC), which constitute the second bottom layer in Figure 1, are more suitable to such systems and have been the focus of many works, as summarized in [16]. The advanced controllers developed recently show better uncertainty handling and stability, as shown in [17] for example, but are still used to follow the logic control rules to operate the solar thermal plant. An example of such

control rules is to maintain a constant temperature at the outlet of the solar field. It has been shown in [18] that allowing a variable outlet temperature could reduce the dumping of solar energy when the solar irradiation is not high enough to reach the target temperature but still allows the production of valuable solar heat.

Thus, replacing the logic control rules by optimized trajectories can improve the solar thermal plant operation. Trajectories are here defined as transient set points, with a value at each discretization point chosen, to be tracked by controllers. A first possibility is to integrate an economic objective into the controllers, as introduced by [19]. Instead of tracking trajectories determined by heuristics, the advanced Model Predictive Controller (MPC) minimizes the operational cost of the solar thermal plant. This has been applied to solar systems in [20] and [21] for instance, to reduce the need of auxiliary energy to satisfy the demand. Although the performances of the solar systems were improved in these two studies, the methodology presents a major drawback: the computational time of the economic optimization has to be shorter than the control sampling time. Thus, a short time horizon is required, along important simplifying assumptions in the control model. This can deteriorate the solar thermal plant operation, especially the storage management policy which requires a longer term strategic vision [22]. Decoupling the control task and the economic optimization might help to overcome these challenges. The economic optimization can be done in the top layer in the hierarchical optimal operation of a system (Figure 1), which is planning, an economic Dynamic Optimization (DO) using a longer time horizon. DO has been studied in [23] and optimal trajectories for all the flow rates in the different parts of a non-concentrating solar thermal plant were determined. Weather forecasts were used to plan the operation. Thanks to this methodology, the operating costs of the plant were reduced by 2.1%, mostly thanks to a decrease in pumping power. In [24], the energy mix of a solar DHN was optimized and an increased share of renewable energy was obtained. However, the solar thermal plant used was not modeled precisely. Dynamic optimization has been more often studied for Concentrated Solar Power

(CSP) plants. In this case, the solar heat produced is at a temperature high enough for electricity generation and TES is used to shift the electricity production depending on the demand and the variable electricity price throughout the day. The optimal operation of a CSP plant was determined a day ahead using weather and electricity price forecasts in ([25], [26] and [27]) with increased revenues from electricity selling. Similarly, the backup fossil fuel consumption of a hybrid gas and solar power plant was reduced with DO in some studies ([28], [29], [30], [31]). All these works improved the solar thermal plant operation with DO, using forecasts. However, the methodology was not tested on a real system undergoing actual environmental conditions which might differ from the uncertain forecasts. The optimal operation determined offline, without adaptations to the actual conditions, can become sub-optimal and the controllers might even fail to track the optimal trajectories if the real-time values differ too much from the forecasts. An intermediate level in the hierarchical operation of a system between control and planning is Real-Time Optimization (RTO), see Figure 1. This layer adapts the optimal operation to the current disturbances, measured on the plant along the state of the system, and passes the optimal trajectories to the controllers of the plant. For dynamic systems, Dynamic RTO (DRTO) can be applied [32]. This is more suitable for solar thermal plants with TES since the elements in the plant have various dynamics preventing the system to ever reach steady-state. DRTO has been widely studied in the last decades for various processes such as a batch reactor [33], a waste water treatment system [34] or a house heating system with storage [35]. In all of these applications, the optimization methodology needs to adapt to disturbances (for example the outdoor temperature and the energy price in [35]) while minimizing the operating cost. DRTO has recently been applied to the solar field of a CSP plant in [36]. Only the flow rate in the solar field was optimized, and no storage was included in the study. But it showed promising performances, with a good uncertainty handling. In another study, the flow rate between a short term and a long term storages in a solar DHN system was optimized in real-time, using weather forecasts and a rolling time horizon of 48 hours, for a year [37]. To

implement the economic optimization in real-time, several simplifications were made: the flow rate is discretized in blocks of 4 hours with a single value and a simple nonlinear model is used. The methodology led to a reduction in electricity consumption of the pumps and thus to lower operating costs. These last two studies had only one flow rate in the solar thermal plant as optimization variable. To optimize the operation of a complete solar thermal plant including thermal storage in real-time, the time horizon should be reduced. However, this would deteriorate the storage management policy, which needs a longer term strategic vision. Hence, it might be better to decompose the optimization in two hierarchical levels to improve storage management [22], by using planning to send information to the DRTO level, as shown in Figure 1. In [38], a hierarchical optimization methodology was applied to a solar thermal plant. The upper level is a planning phase, used for storage management, benefiting from a longer term strategic vision and using weather forecasts. The planned stored energy is passed to a DRTO level optimizing the flow rates in the different parts of the plant. The DRTO objective function is to minimize the operating costs of heat production in real-time while tracking the storage state determined during planning. This methodology has been tested in a simple case study with artificial disturbances and constant heat demand, over only one day, using a shrinking time horizon for the DRTO. The methodology showed improved performances (lower operating costs, increase in solar share) for the solar thermal plant compared to DO, without deteriorating the storage management policy significantly. This is, to the best of our knowledge, the only study where the DRTO of a complete solar thermal plant with storage was investigated.

### *1.3. Paper contributions and organization*

This literature review, which is presented in more details in [39], shows a lack of studies focusing on the DRTO of a complete solar thermal plant. The present paper aims at continuing the work conducted in [38] by applying the DRTO methodology with storage management to a more realistic case study. The main objective of this study is to determine the best way to integrate storage

management in the DRTO objective function for different scenarios. Hereafter are some new features of the research conducted in this paper:

- All independent flow rates in the different parts of the plant are optimization variables, with a value at each time discretization point.
- A variable daily heat demand is considered.
- Real data are used for the weather forecasts and disturbances, allowing a realistic online testing of the methodology.
- The method is tested in simulations over 96 hours.
- A planning phase is used for storage management.
- A rolling time horizon of 12 hours is used for the DRTO.

The remaining parts of the paper are organized as follows. Section 2 presents the solar thermal plant considered and its numerical model. Section 3 presents the input data used in the methodology. Section 4 explains the hierarchical optimization methodology developed. Section 5 details the case studies used to test the methodology. Section 6 presents the results obtained for the various case studies and analyzes the storage management strategies for each case. Finally, Section 7 provides some guidelines regarding storage management in a DRTO methodology for a solar thermal plant. It also gives some perspectives for future work.

## **2. Solar thermal plant description and modeling**

### *2.1. Presentation of the system studied*

The solar thermal plant layout considered in this work is presented in Figure 2. It corresponds to the initial design of a solar thermal plant provided by our industrial partner NEWHEAT, French specialist of large-scale solar thermal plants (<https://newheat.com/en/>).

Here are the main elements of the plant and their typical operation strategies:

- Production loop
  - Solar field made of 15 loops with 12 flat-plate collectors each, representing a total area of 2873m<sup>2</sup>.
  - Fluid composed of 70% of water and 30% of glycol.
  - Recirculation loop accelerates the warm-up phase of the solar circuit by by-passing heat exchanger 1.
  - Standard operation: operation of the solar field operation starts when the solar irradiation exceeds a threshold, 200W.m<sup>-2</sup> for instance. Once warmed-up, the outlet temperature of the solar field is maintained constant by adjusting the flow rate.
- Secondary circuit
  - Storage tank: stratified water tank of 500m<sup>3</sup>.
  - Fluid: water.
  - Dilution possible before heat exchanger 2 to avoid exceeding heat demand.
  - Standard operation: the storage tank is by-passed when the heat production and consumption coincide, any excess heat is charged, and as soon as the heat demand cannot be met, the storage tank is discharged.
- Consumer loop
  - Consumer gas backup burner
  - Ensures heat demand is met, by raising the consumer stream temperature to the target temperature after collection of solar heat.
  - Gas consumption participates to operating costs.
- Heat exchangers
  - 2 heat exchangers to connect the circuits.

- Plate heat exchangers (common choice for low temperatures because of their compactness, efficiency and adaptability [40]) made of 97 plates of  $1.5\text{m}^2$  each.
  - Standard operation: equality of calorific fluxes  $\dot{m}C_p$  in both sides of heat exchanger.
- Variable speed pumps
  - Three-way valves

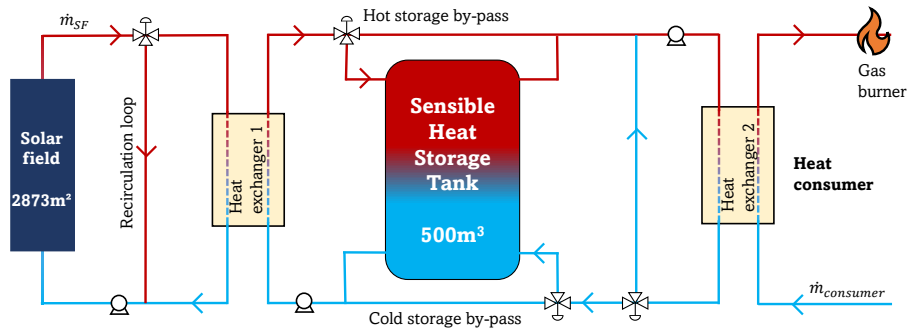


Figure 2: Architecture of the solar thermal plant

As explained above, there are different operational modes in the solar thermal plant depending on the storage utilization (charge, discharge, by-pass) and the temperature adjustment through the recirculation pipe and dilution pipe. Thus, the solar thermal plant operation presents various degrees of freedom which is promising for optimization. Replacing the logic rules detailed previously by an optimal operation might improve the solar thermal plant operation by extending the supply of solar heat for example.

## 2.2. Modeling of the solar thermal plant

The solar thermal plant undergoes variations in both the energy source and the heat demand. Thus, the system is intrinsically dynamic. Moreover, the characteristic times of the elements of the system are different: the solar irradiation varies rapidly while the storage state varies on a slow time scale. Therefore,

we chose a transient model to represent the solar thermal plant. Furthermore, nonlinear phenomena take place in the system. For instance, both the energy transferred and the temperature level of that energy are important to characterize the solar thermal plant operation. Hence, temperature and flow rates appear together in power terms. Linearization of the model would be difficult because there are several operating points [14]. Thus, the model chosen is nonlinear. The model used was originally developed in [23]. An experimental validation of the models was also conducted in the above mentioned paper, using data from a real solar thermal plant in operation. A few changes have been made to the original model, in the solar field and the storage tank, and are detailed in [38]. The optimization methodology developed is for a real-time application so it requires a real system to test it. In this work, the method will be tested on a detailed simulation model set up to represent the real unit. Therefore, both a detailed model and a simplified model for optimization are required. Both models were developed and described in [38]. The main assumptions and equations used for each element of the solar thermal plant are reminded in Appendix A.

There is one difference between the model presented in [38] and the model in the present paper: the spatial discretization scheme used for the storage tank in the simulation model has been replaced by Orthogonal Collocation on Finite Elements (OCFE). Indeed, OCFE ensures a better accuracy in reduced computational times in this case [41]. Hence, two 1D models for the storage tank are used in this paper. Firstly, a model involving finite volume discretization over 10 computational cells, which neglects natural convection, and which is used for optimization purposes. The second model is based on spatial discretization using OCFE, with 15 elements composed of 25 collocation points, and is used as a representation of the real system in the "simulation model". Temperature inversions are corrected regularly. These differences in modeling are representative of a real application since the optimization model cannot perfectly represent the real system. Thus, it is appropriate to test the DRTO methodology using a simplified model for optimization and a detailed model for simulating the real system behavior. However, these differences in modeling should be kept in mind

for the analysis of the case study results.

### 3. Input data

The heat demand and the weather forecasts are the inputs of the optimization problem. The methodology is applied to a detailed simulation model representing the real plant, which undergoes the real weather and heat demand. Our methodology will be tested in a realistic case study and the environmental conditions are real values for the city of Trappes (78), France (coordinates: 48° 46' 39.0000" N, 2° 0' 9.0000" E).

#### 3.1. Weather data

The four parameters used in our model are the following: the Global Horizontal Irradiance (GHI), the Direct Normal Irradiance (DNI), which are both used to compute the solar energy collected in the solar field, the ambient temperature and the wind speed, which are used to calculate the heat losses in the different parts of the solar thermal plant, with the global heat transfer coefficient depending on the wind speed. As explained in Section 1, weather forecasts are useful to plan the optimal solar thermal plant operation ahead of time. The actual measurements of the environmental conditions might differ from the forecasted values and that will impact the actual plant operation. Both forecasted and measured hourly values for the four parameters of interest at the chosen location were provided by Météo-France (<https://meteofrance.fr/>) for the whole year of 2021. The weather forecasts are obtained thanks to Météo-France's ARPEGE model with a new run every 6 hours, providing updated forecasts. The time horizon of the forecasts is up to 103 hours. These forecasted values will be used in the optimization algorithm to compute the optimal operation of the solar thermal plant. The same 4 parameters of interest are measured with a meteorological station in Trappes. These measurements are public data available on request on the following website <https://publitheque.meteo.fr/okapi/accueil/okapiWebPubli/index.jsp>. These measurements will be used

to represent the actual solar thermal plant operation and will allow the testing of our methodology.

### 3.2. Heat demand

The heat consumer considered is a DHN, that could supply heat to various industrial, commercial and residential buildings [42]. Inside the buildings, heat is mostly used for space heating in winter and domestic hot water. Hence, the consumer demand varies seasonally but also daily. Since it is not easy to acquire public data on a DHN heat consumption, the heat demand will be artificially constructed. To simplify this study, an averaged daily heat demand profile was used for every day of the year considered, based on the profile in [43] for a residential DHN. In order to build a heat demand profile consistent with the design of the solar thermal plant, the demand from [43] was adjusted to ensure the supply of heat during two days relying only on a full storage tank at 80°C. The variable daily profile obtained is plotted in Figure 3, with a peak in the demand around 8am and a lower demand around 4pm.

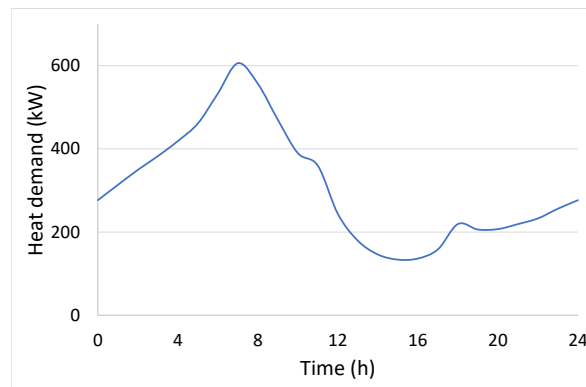


Figure 3: Heat demand profile for a day

We chose a simplified representation of a DHN heat demand, considering a variable flow rate on the consumer side of Heat Exchanger 2  $\dot{m}_{consumer}$  but fixed inlet temperature and target temperature. In a real system, both temperatures also vary. The return temperature of the DHN, which enters Heat Exchanger

2 on the consumer side in Figure 2, is fixed:  $T_{consumer}^{in} = 55^{\circ}C$ . The target temperature is also fixed:  $T_{demand} = 65^{\circ}C$ . The variable flow rate  $\dot{m}_{consumer}$  is computed as follows:

$$\dot{Q}_{demand} = \dot{m}_{consumer} * Cp * (T_{demand} - T_{consumer}^{in}) \quad (1)$$

While  $\dot{m}_{consumer}$  and  $T_{consumer}^{in}$  are both inputs of our model, the temperature at the outlet of heat exchanger 2 on the consumer side is an output which will be impacted by the operational strategy of the solar thermal plant. This temperature should be as close as possible to the target of  $65^{\circ}C$  without ever exceeding it. The gas burner will provide additional heat to reach the target temperature if necessary.

The heat demand is considered variable but perfectly known in advance in this work, which means that it will not be affected by any disturbance during the real-time operation of the solar thermal plant. However, similarly to the uncertain weather forecast presented in subsection 3.1, an uncertain heat demand could also be taken into account with our methodology.

## 4. Optimization methodology

### 4.1. Two-level algorithm

The objective of our methodology is to determine the optimal flow rate trajectories in the different parts of the plant ensuring the lowest operating costs and satisfying the heat demand. As explained in Section 1, storage management in a solar thermal plant might be improved by decomposing the optimization into two hierarchical levels. In our methodology, the first optimization layer, called planning, is in charge of determining the best storage management policy and the second optimization layer, called DRTO, is in charge of the optimal operation of the solar thermal plant. The optimization model is used for both planning and DRTO. Our real-time methodology is tested on a simulation model, which represents the actual solar thermal plant behavior, assuming perfect tracking of the optimal trajectories. The two-layer optimization

methodology is presented in Figure 4. It corresponds to the two upper levels of the hierarchical structure of control and decision making in a plant, presented in Figure 1.

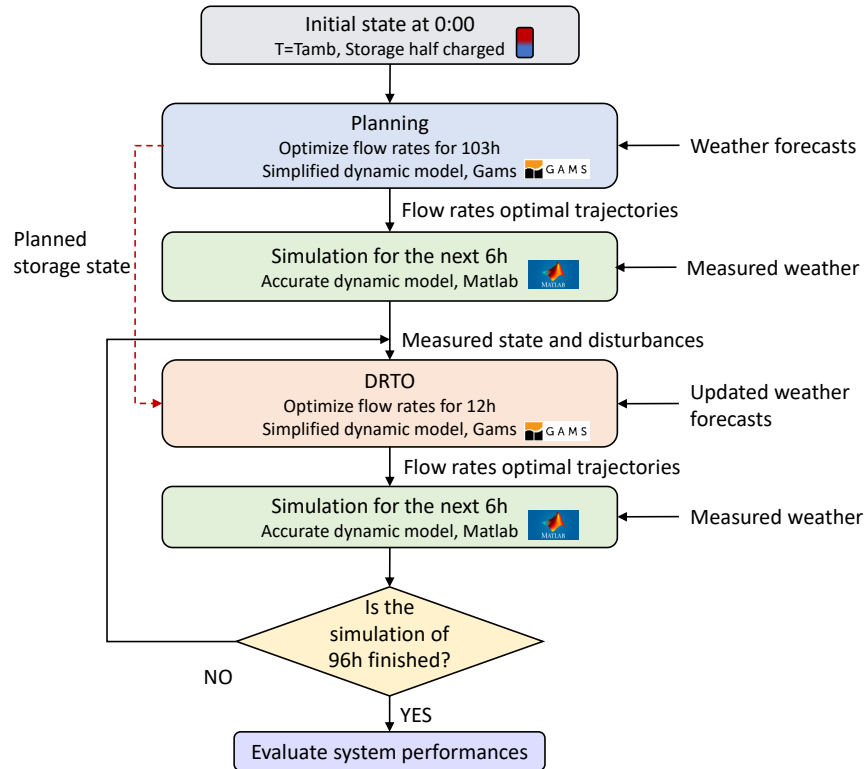


Figure 4: Algorithm for the two-level optimization strategy

At the initial time of the simulation, the storage tank is half charged and all other components of the system are at ambient temperature. At first, the planning phase is run, with a time horizon of 103 hours corresponding to the time horizon of the weather forecast. More details on this step are provided in subsection 4.2. For the next 6 hours, the simulation model will follow the optimal trajectories for the flow rates determined during the planning phase. After 6 hours, an updated weather forecast is available, allowing the start of the real-time adaptation of the optimal operation. After this time, the planning

phase will only be used for storage management, if needed. A new DRTO is run every six hours using a new updated forecast and a time horizon of 12 hours, discussed in subsection 6.4. Details on the DRTO step are provided in subsection 4.3. Between each DRTO run, the behavior of the solar thermal plant will be simulated using the real weather. At the beginning of the DRTO run, the actual state of the system, obtained in the simulation model, will be passed to the optimizer, providing feedback to the DRTO level. The simulation part of the methodology is presented in subsection 4.4. In a real implementation, this methodology would be repeated continuously, with a new planning phase computed regularly, in order to optimize the operation of the solar thermal plant throughout the year. In this work, the planning phase is only computed once and the simulation testing the methodology ends after 96 hours because there is no planned storage state available for the next DRTO.

#### *4.2. Planning*

The planning phase is an offline dynamic optimization with an economic objective function, taking weather forecasts as inputs, following the method developed in [23]. The degrees of freedom in this optimization are the 6 independent flow rates in the different parts of the solar thermal plant. The dynamic model presented in Appendix A is discretized over the whole time horizon, to transform the Differential Algebraic Equations (DAE) into a system of pure algebraic equations that will be solved as a NonLinear Programming (NLP) problem. The time discretization is done with orthogonal collocation on finite elements, following the method in [44], with elements of 1 hour, each containing 9 collocation points. This time discretization was found appropriate in [23]. Using this time discretization, the planning phase takes between 2 and 4 hours to converge to an optimal solution on a laptop with the following characteristics: Intel Core i7-1065G7 1.3GHz. The objective function (OF) to be minimized is the operating costs of the heat production, which entail the electricity consumption of the pumps in the solar thermal plant and the gas consumption of the back up burner. An economic value is given to the stored

energy at the end of the time horizon since this energy could be used after the end of the optimization time span, and thus cut down the gas consumption in the future. In order to obtain smooth optimal trajectories for the flow rates, reducing pumping effort and aging of the equipment, an additional term  $\Phi_{var}$  (explained in [38]) is added to the OF with a weight  $\gamma_{var}$ . This weight is adjusted to obtain a good compromise between good economic performances of the plant and smooth trajectories. The formulation of the dynamic optimization problem is presented hereafter:

$$\min_{free \dot{m}} OF_{eco} - \gamma_{var} \Phi_{var}, \text{ with} \quad (2)$$

$$OF_{eco} = -GasPrice \int_0^{t_f} \dot{Q}_{gas}(t) dt - ElecPrice \int_0^{t_f} \dot{P}_{elec}(t) dt + 0.7 HeatPrice E_{stored}(t = t_f) \quad (3)$$

The prices used in the cost objective function are the following:  $GasPrice = 80\text{€}/\text{MWh}$ ,  $ElecPrice = 130\text{€}/\text{MWh}$  and  $HeatPrice = 25\text{€}/\text{MWh}$ . These prices are orders of magnitude that are specific to a location and time (here France in 2020 [45], [46]) and are here considered constant but could vary throughout the day. The chosen prices impact the optimal operation of the solar thermal plant but still allow a general discussion on the preferred optimization strategy for improved storage management. Since the stored energy will decrease in quality over time before it is supplied to the consumer, due to heat losses and imperfect heat transfer, a weight of 0.7, which was found to be appropriate by [23], affects its associated economic benefits.

There are operational constraints in the dynamic optimization problem ensuring a safe operation:

- $T \leq 95^\circ C$  for all temperatures, to avoid overheating and boiling of the fluid, which would damage the equipment
- The pumps have discontinuous operating modes. The flow rate in each

pump is defined as follows by the manufacturer guidelines to prevent aging:

$$\left\{ \begin{array}{l} \dot{m} = 0 \text{ (corresponding to the pump turned off)} \\ \text{or} \\ 0.3\dot{m}_{max} \leq \dot{m} \leq \dot{m}_{max} \text{ (corresponding to the pump turned on,} \\ \text{with } \dot{m}_{max} \text{ determined by the pump specifications)} \end{array} \right.$$

Sigmoid functions and Big M formulations are used to represent the discontinuous operation, similarly to the example in Appendix A.6.

- $T_{consumer}^{out} \leq T_{demand}$  forbidding exceeding the target temperature ( $T_{consumer}^{out}$  is the temperature of the consumer stream after collecting the solar heat)

The solver CONOPT is used in software GAMS to solve the dynamic optimization problem. The trajectories for the flow rates are initialized with standard operating strategies, ensuring that the local optimum found by CONOPT can be implemented on the actual solar thermal plant. However, the standard operating strategies might not always lead to the respect of all the constraints detailed above. In order to ensure the respect of the constraints and the convergence of the optimization algorithm, the constraints are added progressively. Here are the four steps leading to an optimal solution:

1. Simulate with standard operating strategies, with an upper bound of 120°C for all temperatures and no constraint on the heat demand. Here, there are no degrees of freedom since the flow rates are fixed by the standard operating strategies, and no objective function.
2. Minimize the overheating at the outlet of the solar field, which is the warmest zone of the solar thermal plant at the temperature  $T_{SF}^{out}$ . This first optimization is formulated as follows:  $T_{SF}^{out} \leq 95 + \lambda_{overheating}$  and the objective function is to minimize the scalar  $\lambda_{overheating}$ .
3. Minimize the heat demand excess. Here, all temperatures are limited to 95°C and the optimization problem is the following:  $T_{consumer}^{out} \leq 65 + \lambda_{demand}$  and the objective function is to minimize the scalar  $\lambda_{demand}$ .

4. Minimize the operating costs of the plant, respecting all the operational constraints.

In the DRTO methodology developed in this work, the planning phase can provide the storage management policy, in terms of stored energy throughout time, to the next optimization level. Indeed, the longer time horizon used for planning allows a better strategic vision for the use of storage.

#### 4.3. DRTO

The DRTO level corresponds to the real-time adaptation of the optimization methodology, adapting the operational strategy to disturbances and updated forecasts. Each new DRTO run, performed every 6 hours, retrieves its initial state from the simulation model (as explained in the next subsection). Thus, the new optimal operational strategy is adapted to the current situation. In [47], update frequencies of 24 hours and 6 hours were compared for the optimal dispatch of a CSP plant and a 5% increase in plant revenue was achieved when using a frequency of 6 hours. Thus, 6 hours seems appropriate. The DRTO is an economic dynamic optimization and its formulation is very similar to the planning phase, using the same model. There are a few differences between the two optimization layers, which are detailed hereafter. First, the time horizon is shorter than the planning phase, with the same time discretization. 12 hours are chosen and this choice is further discussed in subsection 6.4. The time horizon should be longer than the control horizon to benefit from a better strategic vision. It also has to be short enough to allow real-time implementation and ensure that the forecasts used are accurate ([26], [27]). With 12 hours, the DRTO takes a maximum of 7 minutes to converge (same laptop as the one used for the planning phase), which is appropriate for a real-time implementation. The objective function is to minimize the same operating costs, however the term on the storage utilization might be different. For the DRTO level, three possibilities will be discussed in Section 6 and are described below:

- DRTO E (purely Economic): excludes storage contribution from the DRTO objective function.

- DRTO M (Maximum storage): uses the same approach as in the planning phase, namely maximizes the stored energy at the end of the DRTO time horizon.
- DRTO P (following Planning): relies on the planning phase. The aim of the DRTO level is to adapt the operational strategy to the current disturbances while trying to follow the plan established previously, based on weather forecasts and a long term strategic vision. To achieve that, the OF incorporates a term minimizing the difference between the planned and the actual stored energies at the end of the DRTO time horizon. An economic value is given to the non-respect of the plan, by multiplying the difference by the price of gas and a weight  $\omega = 0.5$  adjusted in [38]. This represents the fact that the energy that should have been stored but which indeed has not been, will be replaced by gas later. The weight chosen achieves a good compromise between the tracking of the planned storage state and the lowest operating costs. This term is written as follows:

$$\omega \cdot \text{GasPrice} \cdot |E_{\text{stored planning}}(t = t_f \text{ DRTO}) - E_{\text{stored DRTO}}(t = t_f \text{ DRTO})| \quad (4)$$

A similar objective function was used in [47] in a MILP problem for optimal dispatch of a CSP plant and the authors adjusted the weight depending on the season, with higher values in winter when solar irradiation is more variable. This could be explored in future work.

These three possibilities for the DRTO objective function will be compared in the results in Section 6.

#### 4.4. Simulation

Since the methodology developed is a real-time methodology, it has to be tested online on an actual plant. In this work, we use a simulation model solved in MATLAB to represent the actual behavior of the system undergoing the real weather conditions. The dynamic model for simulation takes the optimal trajectories of the flow rates as an input. It forms a DAE system with no degrees

of freedom, that is solved with solver ode15s, to compute the temperatures in all parts of the solar thermal plant. As mentioned earlier, perfect control is assumed, so no controllers are taken into account in the simulation model and the flow rate trajectories are perfectly tracked. The simulation model provides feedback to the DRTO algorithm. Before each new DRTO run, the current system state is retrieved from the simulation and fed to the optimization. No state estimation and data reconciliation steps are included in the methodology. We assume that all states are perfectly measured in first approach. As explained in subsection Appendix A.3, the simulation model uses a more precise representation of the storage tank. By starting regularly with the actual system state, the DRTO algorithm reduces model error propagation due to simplifying assumptions in the optimization model, compared to offline dynamic optimization.

The methodology described above has been tested in some case studies, presented hereafter.

## 5. Case studies

Two distinct time periods will be used in these case studies to show different behaviors of our optimization methodology. In order to choose the time periods, the MAPE (Mean Absolute Percentage Error) between the forecasted and measured GHI are compared for each day of the year 2021 at 12am and for the next 103h, corresponding to the forecast time horizon.

### 5.1. July

The first test period starts on July 19<sup>th</sup> and corresponds to the smallest MAPE of the year (1.2%), meaning that the forecasted GHI is very close to the measured GHI. This is shown in Figure 5 where the forecasted and measured GHI for the next 103 hours, starting at 12am (t=0h), are plotted. The general shape of the GHI is well predicted with only small discrepancies. The measured GHI tends to have a slightly lower maximum value than the forecasted GHI. Overall, this forecasted GHI, which will be used in the planning phase,

is accurate. The forecasts are updated every 6 hours. In this test case, the updated GHI, which will be used for each new DRTO, are very similar to the one determined at 12am on July 19<sup>th</sup>. Based on this observation, we expect our optimization methodology to only lead to slight real-time adaptation.

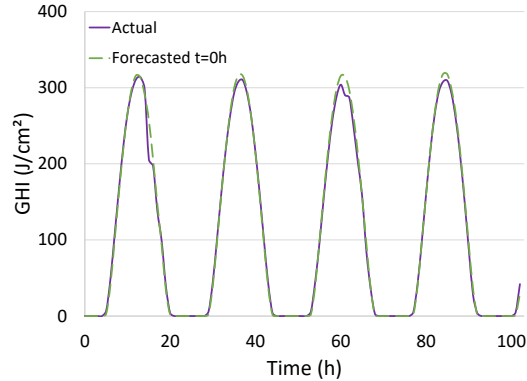


Figure 5: Actual and forecasted global horizontal irradiance for the test period in July

## 5.2. May

The second test period corresponds to a large MAPE (11.2%) for May 12<sup>th</sup>. Larger values were observed in the winter but they correspond to very low solar irradiation levels which are less interesting because the solar thermal plant would barely be operated. The forecasted GHI at 12am ( $t=0h$ ) and the corresponding measured values are plotted in Figure 6 in dashed green and solid purple lines respectively.

We observe that the solar irradiation on the second day is greatly underestimated by the forecast at 12am, which will be used for the planning phase. This underestimation is corrected in the updated forecasts, provided every 6 hours and used at the DRTO level. For instance, the forecasted GHI on May 13<sup>th</sup> at 12am ( $t=24h$ ) is plotted in Figure 6 as well, in dashed orange line. This new forecast does not underestimate the actual GHI as much as the one predicted one day earlier. However, discrepancies between the forecasted and measured

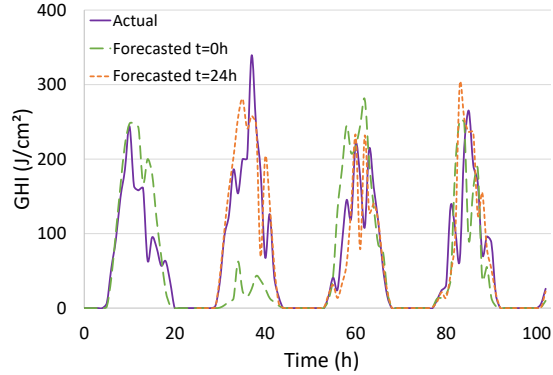


Figure 6: Actual and forecasted global horizontal irradiance for the test period in May

GHI remain because the solar irradiation is quite variable each day during this time period and those fast variations are not well predicted.

### 5.3. Comparison of several optimization strategies

As explained in subsection 4.3, different possibilities to incorporate storage management in the DRTO objective function are explored in this work and will be tested in simulations in the two case studies (July and May) presented earlier and compared. The comparison will also be made to a simulation following the trajectories determined during planning, which is an offline dynamic optimization. This is summarized in Figure 7.

## 6. Results and discussion

The 4 optimization strategies will be compared using the two different time periods chosen. The results analyzed are simulation results since they represent the real behavior of the system following an optimization strategy. The optimal trajectories (6 transient mass flow rates) obtained with the different strategies will be compared directly as well as the resulting temperatures in the different parts of the plant computed by the "simulation model". Performance criteria will also be computed over the whole simulation horizon. The criteria are the following:

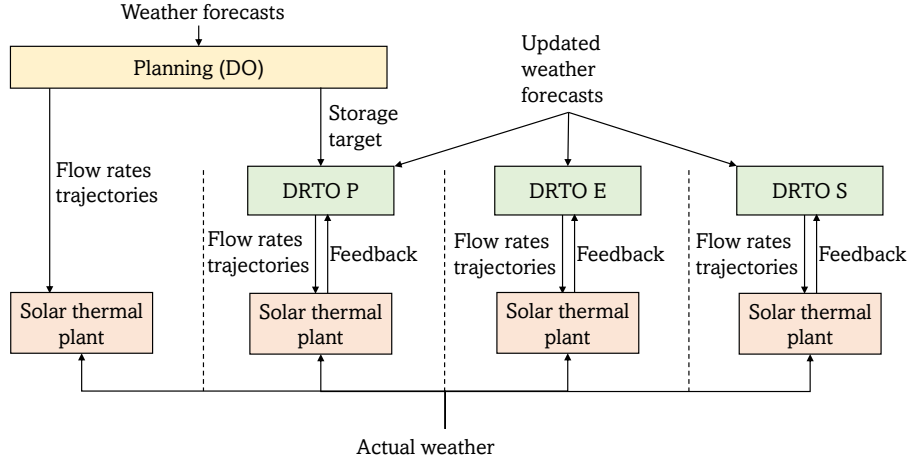


Figure 7: Comparison of several optimization strategies

- $E_{supplied}$ : quantity of solar heat supplied to the consumer, either directly from the solar field or from the storage tank, at a temperature lower than the target temperature. Any excess heat is not included.  $E_{supplied}$  should be as high as possible to reduce gas consumption in the back-up burner in the consumer circuit.
- $E_{elec}$ : electric consumption of the pumps.
- $C_{tot}$ : total operating costs of the plant (electricity and gas consumption)
- $E_{stock\ final}$ : quantity of valuable energy (above the consumer return temperature of 55°C) inside the storage tank at the end of the simulation.

The heat demand presented in subsection 3.2 corresponds to a total of 29.82MWh for the whole 96 hours.

### 6.1. Small disturbances: July test period

At first, the test period in July was chosen. Since the weather is correctly predicted for the whole time horizon and there is high solar irradiation available, this represents an ideal case. Indeed, we expect all strategies to satisfy the heat demand. This will allow us to verify that DRTO does not deteriorate the solar

thermal plant performances compared to DO due to the frequent updates in the optimal trajectories and the lack of strategic vision.

The performances of the four simulations, following the trajectories determined with the four optimization strategies, are summarized in Table 1. Firstly, we observe that the energy supplied is lower than the heat demand of 29.8MWh for all methods. The difference is the largest for DO (about 16%). There are two reasons explaining the differences. First, the solar irradiation is slightly overestimated for most days, as shown in Figure 5. The updated forecasts, provided every six hours for each new DRTO, are slightly more accurate but they still tend to overestimate the GHI. Thus, when using the actual weather, the heat production is reduced and the demand is not perfectly satisfied. The second reason are the model and resolution differences between the simplified optimization model and the detailed simulation model representing the real plant. In order to assess the effect of the difference in models only, the 4 optimization strategies were compared in a test with undisturbed weather. This means that the real-time weather does not deviate from the forecasted weather in this test and the same weather inputs were used at each level of the optimization algorithm: planning, all DRTO and simulation of the real plant. Even without any disturbances in the weather, the heat demand is still not perfectly met in the four simulations, and the discrepancy is larger for DO ( $E_{supplied}$  is 7.5% lower than the demand for DO and about 5.5% lower for the three DRTO strategies). This stems from the differences in modeling, mostly for the storage tank as detailed in Appendix A.3, and in resolution methods, mostly time integration, as explained in Section 4. Although the heat demand is met in the optimization model, when the trajectories are used on the detailed simulation model, the performances of the simulated plant are slightly different than expected, they were reduced in this test. Since the DRTO method starts every six hours with the actual state of the system, retrieved from the simulation model, it reduces the model error propagation.

DO is the most expensive strategy since it needs more gas to complete the heat demand. The electricity consumption of the pumps can also be compared

in Table 1 for the case with the real weather data. We observe a lower electricity consumption for DRTO E. This has to be analyzed along with the stored energy at the end of the simulation. It is the lowest for DRTO E since there is no objective on storage. This strategy collects the minimum solar energy required to satisfy the heat demand, reducing the flow rates in the plant, thus leading to lower electricity consumption. Therefore this strategy is the least expensive in this case. However, the stored energy is lower, which could lead to more gas consumption in the future. DRTO P and DRTO M show very similar performances, with slightly more energy stored at the end of the simulation for DRTO M. In order to better understand the differences in operational strategies between DO, DRTO E, DRTO P and DRTO M, trajectories for various variables are compared.

Table 1: Comparison of the performances of the simulated solar thermal plant in July using the different optimization strategies

Performance	Simulation performances			
	DO	DRTO E	DRTO P	DRTO M
$E_{supplied}$ (MWh)	24.86	27.94	27.89	27.82
$E_{elec}$ (MWh)	0.18	0.10	0.18	0.16
$C_{tot}$ (€)	419	162	177	180
$E_{stock\ final}$ (MWh)	15.71	10.44	14.32	14.85

The flow rates in the solar field for the four strategies are compared in Figure 8 and the stored energies throughout time are plotted in Figure 9. DRTO E uses a lower flow rate in the solar field over the whole simulation horizon, which leads to lower electricity consumption as explained earlier, and to less solar energy collected and stored. Indeed, in Figure 9, the stored energy for DRTO E is lower than for other strategies for the last three days. The differences in stored energy for the other three strategies are small. The flow rate computed with DO increases day after day. We observe that the stored energy for DO is

lower than the other strategies on day 1, but increases every day, and it is the largest at the end of the 96h. Because it benefits from a longer-term vision, DO tends to store less at the beginning of the 96h time span. This ensures that the storage is not full for as long as possible, leading to a better solar yield because the temperature of the water entering the solar field is lower [5]. Once the end of the 96h time horizon draws near, the flow rate in the solar field is increased, to maximize solar heat collection and storage. DRTO P tends to follow the same trend while DRTO M uses the same flow rate each day, constantly maximizing solar heat production and storage. Figure 10 shows the temperature profile in the storage tank after 12 hours of simulation for DO, DRTO P and DRTO M. We observe that the cold zones for DO and DRTO P are larger than for DRTO M, allowing more storage capacity for the next days. Moreover, the temperature at the top of the storage tank is higher for DRTO P. This is due to the smaller flow rate in the solar field, leading to higher temperatures, and thus higher quality energy stored and leaving more space for future storage needs .

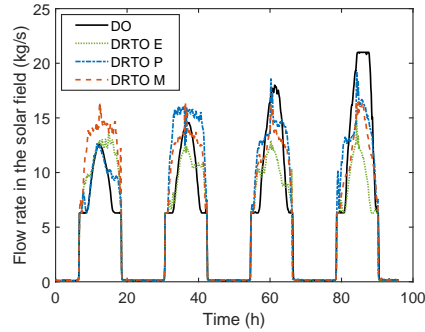


Figure 8: Comparison of the flow rates in the solar field in July

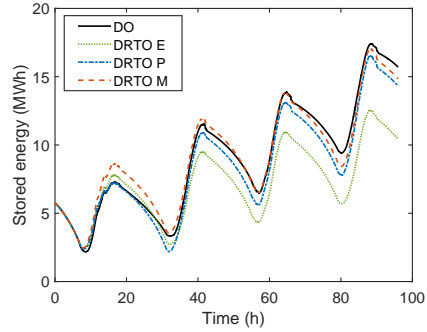


Figure 9: Comparison of the simulated stored energies in July

This case study shows that DRTO still improves the performances of the solar thermal plant even though the disturbances on the weather are very small. In this case, all DRTO strategies led to lower operating costs. DRTO E stored less solar energy, which might affect future operation, but led, at the same time, to the lowest cost for the 96h time span. However, DRTO P and DRTO M,

although using different operational strategies as explained above, led to similar performances for the whole simulation of the solar thermal plant. The next case studies will help to determine which strategy, among DRTO P and DRTO M, should be used in different situations.

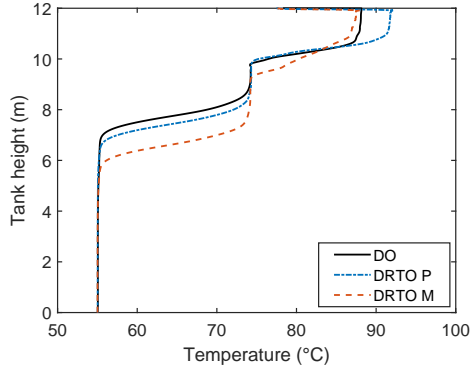


Figure 10: Comparison of the simulated temperature profiles in the tank at 12h

### 6.2. Storage management in mid-season

The second test case is a period in May, typical of mid-season: the solar irradiation is variable, difficult to predict accurately and not high enough throughout the entire day to store sufficient energy to satisfy the heat demand over the entire simulation duration. The performances achieved with the four optimization strategies are presented in Table 2.

First, one can notice that DO is the strategy supplying the least energy to the consumer (about 38% of cumulative heat demand), leading to the highest operating cost for heat production (associated to important gas consumption). This can be explained by the error in the solar irradiation forecast used for the planning phase, as shown in Figure 6. The initial forecast predicted a very low solar irradiation on the second day whereas the next forecasts and the measures actually show a high GHI. Therefore, the optimal operation on day 2 with DO was to shut down the solar thermal plant. No flow rate is circulating in the solar field, as shown in Figure 11 which presents the flow rates in the solar field for the four strategies. Moreover, no heat is supplied to the consumer

Table 2: Comparison of the performances of the simulated solar thermal plant in May using the different optimization strategies

Performance	Simulation performances			
	DO	DRTO E	DRTO P	DRTO M
$E_{supplied}$ (MWh)	11.25	15.22	15.91	17.63
$E_{elec}$ (MWh)	0.20	0.05	0.14	0.11
$C_{tot}$ (€)	1512	1174	1131	989
$E_{stock\ final}$ (MWh)	0.76	0.37	0.82	0.87

because the storage tank was emptied the night before, as shown in Figure 12 which presents the stored energy throughout time for the four strategies. The stored energy even becomes negative due to heat losses, which means that the average temperature inside the storage tank is lower than the reference temperature corresponding to the return temperature of the consumer stream at 55°C. All three DRTO strategies perform better than DO because they use a better estimate of the solar irradiation. They also all use less electricity for the pumps, with DRTO E leading to the lowest electricity consumption. This is due to lower flow rates, for example a lower flow rate is used in the solar field for all three real-time strategies, as shown in Figure 11. DRTO E is the DRTO strategy leading to the lowest amount of energy supplied to the consumer and stored at the end of the simulation. This is because there is no objective on storage and the DRTO algorithm only has a strategic vision of 12 hours. Thus, DRTO E does not store a lot of energy in anticipation of future periods with no or low solar irradiation. This can be seen in Figure 12, where the stored energy on day 1 is the lowest for DRTO E, leading to less solar energy available for the next days. Therefore, it is necessary to incorporate a term on storage management in the DRTO objective function. Finally, for this case study, DRTO M allows to supply more solar heat to the consumer than DRTO P, about 6% more heat demand satisfied, reducing the operating cost by 16%. DRTO P includes a term

in its objective function to minimize the difference between the planned storage state and the actual stored energy at the end of the time horizon. In this test, the planning was determined using inaccurate weather forecasts, especially on the second day. Thus, the planned storage state is not optimal and tracking it in the real-time phase deteriorates the performances of the solar thermal plant. This can be seen in Figure 12, where the stored energy on the second day for DRTO P is low, even lower than DRTO E.

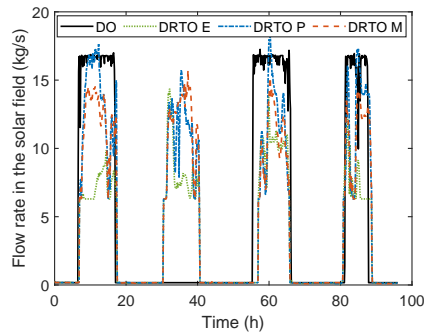


Figure 11: Comparison of the flow rates in the solar field in May

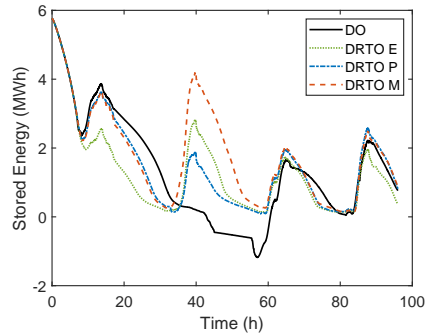


Figure 12: Comparison of the simulated stored energies in May

This is confirmed in Figure 13, which presents the charge flow rate for DRTO P and DRTO M. We observe that the charge flow rates are similar for both strategies on days 1, 3 and 4. However, on day 2, the charge flow rate for DRTO P is reduced because the algorithm tracks the planned storage state determined with a low solar irradiation on day 2.

This shows that using the planning phase for storage management can lead to deteriorated performances for the solar thermal plant if the planning is inaccurate. It would be better to re-compute a new planning whenever the weather data differ too much from the forecasted data used for planning. This requires weather data available often and is computationally expensive. Based on the analysis of both case studies in July and May, maximizing the stored energy at the end of the DRTO time horizon leads to the best performances for the heat production: more solar heat delivered to the consumer and stored in the storage

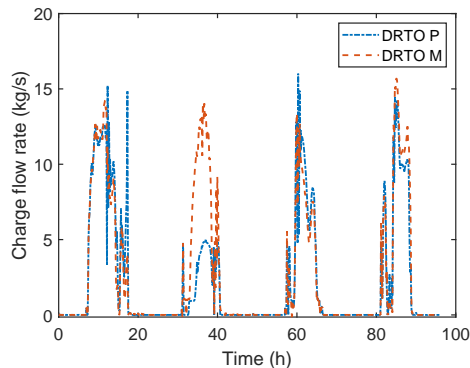


Figure 13: Comparison of the charge flow rates for two DRTO strategies

tank. In this scenario, DRTO M led to an increase of 57% in supplied energy and a reduction of 35% in operating costs compared to DO. So for normal operating conditions, which do not lead to overheating and complete filling of the storage tank, DRTO M seems to be the best strategy, regardless of whether the planning phase is accurate or not. In the next subsection, an extreme scenario leading to overheating will be studied to assess the best storage management strategy in this situation.

### 6.3. Storage management in summer: avoiding overheating

A scenario particularly challenging for solar thermal plant operators is when there are several sunny days in a row in summer and the storage tank is full. The solar thermal plant is exposed to overheating, which means that the temperature in the solar field rises too much, leading to thermal expansion and even ebullition [5]. This situation could damage the solar plant equipment and therefore should be avoided. Generally, the solar thermal plant is designed to meet the heat demand during summer, when the solar contribution is the highest [5]. This should prevent overheating, and back-up heaters will be used in other seasons to complete the demand. This is what was observed in the previous case studies: no overheating happened in July and gas was necessary to satisfy the heat demand in May. Nevertheless, extreme scenarios could still happen, and optimization could help to prevent overheating in these scenarios. In the present case study,

the test period in July is used. However, we now consider that at the initial time of the 96 hours time span, the storage tank is full, with a uniform temperature of  $75^{\circ}\text{C}$ . This corresponds to a stored energy of 11.61MWh. The maximum theoretical capacity of the storage tank is 23.22MWh when the temperature is uniform equal to  $95^{\circ}\text{C}$ , which is the maximum allowed temperature in the system. In reality, the temperature in the system rarely reaches that level and we did consider the storage tank at  $75^{\circ}\text{C}$  full because there is no cold zone. Additionally, the heat demand has been reduced to a maximum of 334kW. This means that in Figure 3, the peak has been reduced to 334kW, which in turns, corresponds to a flow rate of  $8\text{kg}\cdot\text{s}^{-1}$ . The total heat demand for the 96 hours of simulation is 25.09MWh in this case. This modified heat demand was artificially built to increase the risk of overheating. The same reduced demand was used at each level of the methodology: planning, DRTO and simulation. The objective of this case study is to find the best storage management strategy to prevent overheating. There are specific strategies that could be employed to prevent overheating (night cooling in the solar field [5] or defocusing of the solar panels [48] for example) and safety elements are present in the plant to handle overheating without damaging the solar field (expansion vessels, safety valves, drainback systems [40]). These elements and strategies are not included in our solar thermal plant model, so the only way to prevent overheating, if possible, is to use a smart storage management policy.

The four optimization strategies presented in 5.3 have been applied to this extreme scenario. In the case of DRTO M, the DRTO number 9, which starts at 54h did not converge. It corresponds to the middle of day 3, when the solar irradiation is high and after two sunny days during which the storage tank was already filled with hot fluid. When analyzing this convergence fail, we observe that it is due to overheating. At some point during the time horizon, the storage tank is completely full, the solar irradiation is high and the heat demand is not very large. The optimization algorithm is not able to respect both constraints:  $T \leq 95^{\circ}\text{C}$  (no overheating) and  $T_{consumer}^{out} \leq T_{demand}$  (no exceeding of the heat demand). Either more solar heat needs to be evacuated in heat exchanger 2, or

the temperature will rise in the solar field above the safety limits. This has been verified by relaxing either constraint, convergence was obtained in both cases. When moving either of the constraint in the objective function, to authorize the violation of the constraint but penalize it, convergence was achieved but the constraint was indeed violated even with a strong penalization. With the two constraints imposed, the optimization is infeasible and the trajectories for the flow rates that would be provided to the simulation model do not verify all physical equations and operational constraints. Thus, the overall numerical integration process was stopped at 54 hours. All three other strategies converged over the whole simulation time span.

Figure 14 presents the stored energy throughout time for the four simulations following the four optimization strategies. We observe that the stored energy is much more important for DRTO M, more energy was charged during days 1 and 2. At the hour 54, when DRTO 9 fails for the DRTO M strategy, the initial stored energy is 17% higher than the one obtained with the DRTO P strategy. So during the first two days, the DRTO M strategy stores more energy in the tank, as shown in Figure 15. While the three other strategies all use similar charge flow rates, DRTO M uses a higher charge flow rate because its objective is to store as much as possible at the end of each DRTO. In this extreme scenario, this optimization strategy is not suitable because the lack of anticipation leads to an overfull storage tank when the solar irradiation is high, and thus to overheating.

On the first day, all three other strategies lead to the same amount of energy stored, which is the minimal amount. This is because DRTO E does not store additional energy for latter use and DO and DRTO P avoided to store too much to ensure a safe operation for the next days. The simulation with DO presents significantly less solar energy stored than DRTO P (and even DRTO E), although DRTO P follows the storage management policy determined by DO. As explained before, DO stores less energy than expected because it collects less solar energy than expected due to the errors in the forecasts and the model (see subsection 6.1 for the explanations). So the stored energy originally planned in the optimizer, which is the objective used in DRTO P, is larger. This explains

why DRTO P stores more energy than DO. This was also observed in [38].

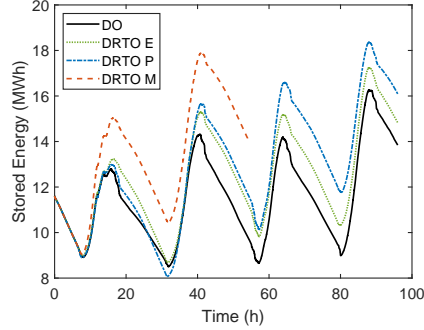


Figure 14: Simulated stored energy in July with reduced heat demand

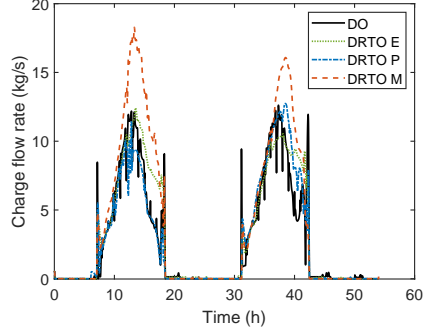


Figure 15: Charge flow rate in July with reduced heat demand

Table 3 presents the performances of the solar thermal plant for the different optimization strategies. The performances of DRTO M are not computed since the overall process is stopped at 54h after an optimization did not converge. Similarly to the results presented in subsection 6.1, DO supplies the least amount of heat to the consumer, 87% of the heat demand, because of the slightly inaccurate weather forecasts and simplifying assumptions in the optimization model.

DRTO E stores less energy at the end of the simulation than DRTO P but the difference is smaller than when the demand was not reduced (only 8% difference compared to the 27% difference in the case study presented in subsection 6.1). The difference is small because there is excess energy every day produced in the solar field since the demand is low, so even DRTO E stored this excess heat. Moreover, DRTO P does not store more energy to avoid overheating. DRTO P still leads to more energy stored starting from day 2 because the storage management policy provided by DO allows more storage towards the end of the simulation, once the risk of overheating is handled. The operating costs for DRTO E and DRTO P are similar, slightly larger for DRTO P because it consumes more electricity.

Overall, DRTO P leads to the best performances in the solar thermal plant,

with low operating costs and a full storage tank at the end of the simulation, without overheating.

Table 3: Comparison of the performances of the simulated solar thermal plant in July when there is a risk of overheating

Performance	Simulation performances		
	DO	DRTO E	DRTO P
$E_{supplied}$ (MWh)	21.76	23.67	23.62
$E_{elec}$ (MWh)	0.15	0.12	0.17
$C_{tot}$ (€)	286	129	140
$E_{stock\ final}$ (MWh)	13.84	14.83	16.09

#### 6.4. Impact of the DRTO time horizon

In this work, a time horizon of 12 hours was chosen for the DRTO. Since the time horizon might affect the operational strategy, a test was conducted to assess its effect. Additional simulations with DRTO using time horizons of 6 hours and 24 hours were run. First, the computational times of one DRTO algorithm for the three different time horizons were compared in Table 4.

Table 4: Comparison of the computational times for one DRTO run for different time horizons

Time horizon (h)	6	12	24
Average time (min)	1	2.5	6
Maximum time (min)	4	7	26

The computational times are averaged for every test period and DRTO strategy. All time horizons could be chosen for a real-time application, with fast convergence on average. A time horizon of 24 hours might lead to long computational times, with a maximum time of 26 minutes found among all cases, but it still remains applicable in real-time given that the update frequency is only

six hours. Thus, the choice of the suitable time horizon depends on the solar thermal plant performances achieved.

Figure 16 shows the simulated stored energy throughout time for the test period in May using DRTO E with different time horizons. We observe that the stored energy is higher when using a longer time horizon because the DRTO algorithm can anticipate the need for stored energy. As a result, the supplied energy is larger and the operating costs of heat production lower for the time horizon of 24 hours. On the other hand, Figure 17 presents the stored energy for DRTO M. For this strategy, the time horizon does not impact the quantity of energy stored throughout time. The performances of the solar thermal plant are not affected by the time horizon significantly. This is because the storage management is incorporated into the objective function and the DRTO algorithm does not need a long term strategic vision to make the most of the storage tank. A similar analysis can be conducted for DRTO P. Based on this observation, a time horizon of 6 hours, which requires the least computational effort, could be satisfactory.

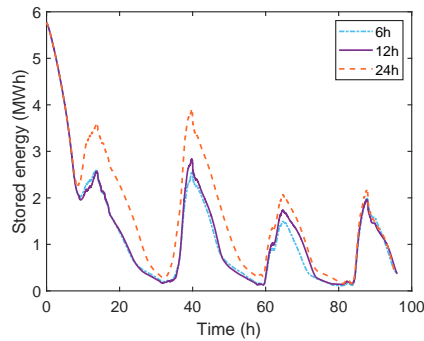


Figure 16: Impact of the time horizon for DRTO E in May

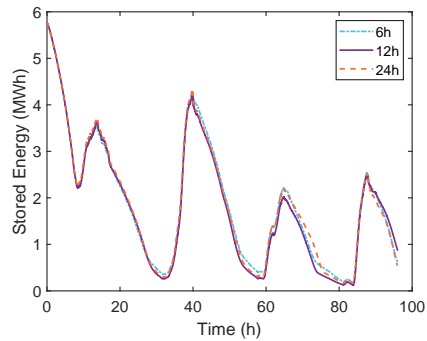


Figure 17: Impact of the time horizon for DRTO M in May

The simulations were also conducted in July, for both the standard and the extreme scenarios. We noticed more frequent overheating when using a time horizon of 6 hours compared to 12 hours, even for DRTO P. Although storage management is determined by planning in this strategy, having a longer time

horizon seems to help avoid overheating in some situations. Therefore, a time horizon of 12 hours is long enough when using a storage management objective, is computationally acceptable and still provides a few hours of strategic vision to the DRTO algorithm.

## 7. Conclusion and Perspectives

In this study an economic DRTO methodology, including a planning phase, for a solar thermal plant was developed and tested online in several case studies. Real data for the weather forecasts and measurements were used. The methodology was tested on a detailed simulation model, representing a large scale solar thermal plant. Firstly, it has been observed that DRTO improves the solar thermal plant performances compared to DO even when the forecasts used for DO are accurate. This is due to the regular update of the system state with measured values, reducing model error propagation. An increase up to 57% in supplied energy and a decrease up to 35% in operating costs were achieved with DRTO compared to DO in a case study with variable solar irradiation and uncertain forecasts. The main objective of this work was to determine the best storage management policy by comparing several optimization strategies. All optimization strategies aim at minimizing the operating costs from gas and electricity consumption, but they treat the storage management differently. From the different case studies, some guidelines for the optimal operation of a solar thermal plant could be formulated:

- The planning phase should be run to determine if there is a risk of overheating in the following days. A risk of overheating could be defined as a saturation of the storing capacity (complete filling of the tank at high temperature) at one point during the DO.
- If there is no risk of overheating for the following days, the DRTO M strategy should be adopted. This means that the stored energy is maximized at the end of each DRTO time horizon. The maximized stored energy will

allow the supply of solar heat later, when no solar irradiation is available, reducing gas consumption for the heat production.

- If there is a risk of overheating, the DRTO P strategy should be adopted. The DRTO P will follow the planned stored energy at the end of each DRTO time horizon. This should avoid overheating by storing energy only if it does not deteriorate the plant operation in the following days.
- A time horizon of 12 hours for the DRTO seems suitable to determine the best operational strategy.
- The planning phase should be updated regularly, especially when the weather forecasts differ a lot from the actual weather conditions.
- Although it did not happen in the case studies presented, the planning phase could fail to converge. Indeed, we showed that the use of planning can help to avoid some overheating situations, but extreme scenarios could lead to overheating predicted even during the planning phase. In this case, the DRTO E strategy should be used because it stores the least energy and collects the minimum amount of solar heat to satisfy the heat demand. Overheating might happen, and safety devices will be activated to protect the solar thermal plant, but DRTO E should reduce the overheating to a minimum. As soon as a new planning phase converges, which means that the risk of overheating can be handled again, the DRTO M or DRTO P strategy should be adopted again, depending on the guidelines above.
- Overheating can still happen even when following these guidelines, but the occurrences of overheating should be very limited. In case of overheating, safety equipment included in the solar thermal plant must protect the system.

In future work, these guidelines could be tested for more case studies, to formulate more precise criteria for the switching between the different DRTO strategies. Moreover, a criterion on the deviation between the forecasts used for

planning and the actual environmental conditions could be formulated to trigger a new planning computation. In this study, the connection between the planning and the DRTO P strategy was to minimize the difference between the planned stored energy and the actual stored energy at the end of the DRTO time horizon. Other possibilities, such as tracking the planned stored energy at a fixed time in the day, sunset for example, could be explored. Finally, future work could focus on improving the models developed, by incorporating the safety equipment used in case of overheating, and add the optimization of these devices in the optimal operation of the plant, and also by modeling non ideal controllers to add them in the detailed representation of the plant.

## Acknowledgements

The project leading to this publication has received funding from Excellence Initiative of Université de Pau et des Pays de l'Adour – I-Site E2S UPPA, a French “Investissements d’Avenir” programme.

## Appendix A. Model equations

### Appendix A.1. Solar field

The chosen model is the one-node capacitance model and is based on the following assumptions: there is no spatial discretization of the temperature inside a collector, no heat losses between the collectors within a loop and the distribution of the fluid between the loops is uniform. The solar field is here represented by a single solar panel with an area  $A_{SF}$  equal to the total area of all the solar collectors. The mean temperature  $T_{SF}^{mean}$  in the solar field is computed with the following energy balance equation [49]:

$$\frac{\dot{Q}_{SF}}{A_{SF}} = \left( \eta_{0,b}(\eta_{sh}K_b(\theta)G_b + K_dG_d) - c_1(T_{SF}^{mean} - T_{amb}) - c_2(T_{SF}^{mean} - T_{amb})^2 - c_5 \frac{dT_{SF}^{mean}}{dt} \right) \quad (\text{A.1})$$

With:

$\dot{Q}_{SF}$  power collected by the heating fluid [W],

$G_b$  direct solar irradiation in the plane of a collector [ $W.m^{-2}$ ],

$G_d$  diffuse solar irradiation in the plane of a collector [ $W.m^{-2}$ ],

$T_{amb}$  ambient temperature [ $^{\circ}C$ ],

$\eta_{0,b}$  collector optical efficiency,

$c_1$  heat loss coefficient in the collector at  $T_{mean} = T_{amb}$  [ $W.m^{-2}.K^{-1}$ ],

$c_2$  temperature dependence of the heat loss coefficient [ $W.m^{-2}.K^{-1}$ ],

$c_5$  effective thermal capacity [ $J.m^{-2}.K^{-1}$ ],

$K_b(\theta)$  incidence angle modifier for the direct irradiation,

$K_d$  incidence angle modifier for the diffuse irradiation,

$\eta_{sh}$  shading effect of a solar field loop onto the next loop.

Inside the collectors, a linear temperature distribution is assumed:

$$T_{SF}^{mean} = \frac{T_{SF}^{in} + T_{SF}^{out}}{2} \quad (A.2)$$

This simplified dynamic model is able to represent the fast variations in the solar field temperature accurately with a reduced computational time.

#### *Appendix A.2. Heat exchangers*

A simple model is used to keep the computational time low while still achieving a good accuracy, considering no spatial discretization. The other main assumptions are:

- no heat losses to the environment,
- no accumulation,
- a uniform distribution of the fluid flow between the channels,
- the same exchange area for every pass,
- a perfect mixing at the end of a pass.

The effectiveness-NTU model is chosen, as described in [50] for example. The three main equations of the model are hence the following:

$$\dot{Q}_{HX} = (\dot{m}C_p)_{cold}(T_{cold}^{out} - T_{cold}^{in}) \quad (A.3)$$

$$\dot{Q}_{HX} = (\dot{m}C_p)_{hot}(T_{hot}^{in} - T_{hot}^{out}) \quad (A.4)$$

$$\dot{Q}_{HX} = \epsilon_{HX}(\dot{m}C_p)_{min}(T_{hot}^{in} - T_{cold}^{in}) \quad (A.5)$$

With:

$(\dot{m}C_p)_{min}$  minimum heat capacity between the two sides of the heat exchanger

$(\dot{m}C_p)_{min} = \min((\dot{m}C_p)_{hot}, (\dot{m}C_p)_{cold}) [W.K^{-1}]$ ,

$(\dot{m}C_p)_{max}$  maximum heat capacity  $[W.K^{-1}]$ ,

$\epsilon_{HX}$  effectiveness of the heat exchanger.

$\epsilon_{HX}$  can be computed with the following equations:

$$R = \frac{(\dot{m}C_p)_{min}}{(\dot{m}C_p)_{max}} \quad (A.6)$$

$$NTU = \frac{U_{HX}A_{HX}}{(\dot{m}C_p)_{min}} \quad (A.7)$$

With:

R heat capacity ratio,

NTU number of transfer units,

$A_{HX}$  total exchanged surface of the heat exchanger  $[m^2]$ ,

$U_{HX}$  global heat transfer coefficient (considered constant equal to  $4000W.m^{-2}.K^{-1}$

in this work to reduce the nonlinearities and speed up the calculations [48]).

The effectiveness for a counter-current flow heat exchanger is then defined as follows:

$$\left\{ \begin{array}{l} \epsilon_{HX} = \frac{1 - \exp(-NTU(1-R))}{1 - R \exp(-NTU(1-R))} \text{ if } R < 1 \\ \text{or} \\ \epsilon_{HX} = \frac{NTU}{1+NTU} \text{ if } R > 1 \end{array} \right.$$

### Appendix A.3. Storage tank

The storage tank considered is a 12 meters high vertical cylinder with a volume of  $500m^3$ . It is a stratified water tank, charged with hot water from the top and with the return cold water entering the bottom. That way, there is limited mixing between the hot zone at the top of the tank and the cold zone at the bottom of the tank [6]. Between the hot and cold zones, there is a high temperature gradient region, also known as thermocline. It is particularly challenging to model a stratified storage tank because it needs a very accurate model to represent the thermocline region. However, such a detailed model can lead to long computational time. A 1D model was chosen in this work to reduce the calculation time. Only the variations of the temperature along the vertical axis of the storage tank are considered. There are several approaches to model a storage tank in 1D, listed in [41] for example, but the solving of the energy balance is more accurate because it is based on physical phenomena. The conservation of energy in 1D, along an ascending vertical axis  $z$  and over a control volume of thickness  $dz$  can be written as follows, assuming constant thermophysical properties for the stored fluid and no heat source inside the storage tank:

$$\rho C_p A_s \frac{\partial T_s(z, t)}{\partial t} + \dot{m} C_p \frac{\partial T_s(z, t)}{\partial z} = A_s k \frac{\partial^2 T_s(z, t)}{\partial z^2} + U_s P (T_{amb}(t) - T_s(z, t)) \quad (\text{A.8})$$

With:

$T_s(z, t)$  temperature inside the tank [C],

$\dot{m}$  resulting flow rate from charging and discharging [ $kg.s^{-1}$ ],

$\rho$  fluid density [ $kg.m^{-3}$ ],

$C_p$  fluid heat capacity [ $J.kg^{-1}.K^{-1}$ ],

$k$  fluid thermal conductivity [ $W.m^{-1}.K^{-1}$ ],

$A_s$  the tank cross-sectional area [ $m^2$ ],

$P$  tank cross-sectional perimeter [ $m$ ],

$U_s$  overall heat transfer coefficient with the ambient [ $W.m^{-2}.K^{-1}$ ].

In order to solve this PDE, it is first converted into an ODE system by using a spatial discretization scheme. The multinode model, based on finite volumes is used for the optimization model. A model with 10 layers was chosen as it provides a reasonable estimate of the temperature profile and the energy stored with very fast calculations [23]. However, the thermocline region is not well represented because of the effect of numerical diffusion [51].

For the simulation model, a more accurate representation of the storage tank is required as the model acts as a virtual replacement of the actual plant to test the methodology. Another spatial discretization scheme was used to convert the PDE into ODE: Orthogonal Collocation on Finite Elements (OCFE) to reduce numerical diffusion. The numerical method is presented in [41] in the specific case of a stratified storage tank. OCFE combines the advantages of both orthogonal collocation, where a limited number of discretization points is needed to converge to the actual differential equation solution, and finite volumes, where the resolution of the system is fast due to the sparsity of the matrix generated [52]. For our model, we chose 15 elements with 25 points each, so 375 discretization points in total.

Natural convection is not represented in Equation A.8 although it might occur in the storage tank during charging [53] or due to heat losses [54]. Natural convection is particularly challenging to be taken into account in 1D models as it involves 3D fluid movements. This phenomenon was neglected in the optimization model to keep it as simple and computationally efficient as possible, avoiding conditional structures [41]. This simplifying assumption leads to temperature inversions inside the storage tank, which would not remain more than a few minutes in the real system. For the simulation model, temperature inversions are corrected regularly by stopping the time integration and computing a new temperature profile which will be used as the initial condition of the next integration period. This new temperature profile is determined by averaging between two temperature profiles, one with reorganized temperatures following the approach from [55] and one with homogenized temperatures following

the approach from [56]. Indeed, the first approach tends to overestimate the stored energy inside the tank while the second one tends to underestimate it [53]. Averaging between both profiles might provide a better estimate of the actual temperature profile in the tank after natural convection took place.

#### *Appendix A.4. Pipes*

Each pipe of the system represented in Figure 2 is modeled in 1D with an energy balance equation, without spatial discretization:

$$\rho C_p \pi A_{pipe} L \frac{dT^{out}}{dt} = \frac{T_{amb} - T^{out}}{R_{th}} + \dot{m} C_p (T^{in} - T^{out}) \quad (\text{A.9})$$

With:

$A_{pipe}$  cross-sectional area of the pipe [ $m^2$ ],

$L$  length of the pipe [ $m$ ],

$R_{th}$  thermal resistance [ $K.W^{-1}$ ], taking conduction in the insulation layer and external convection into account, assuming ideal internal convection and conduction through the wall.

Mass and energy balances are developed at each mixing valve and flow division, neglecting the accumulation and heat losses.

#### *Appendix A.5. Pumps*

The electricity consumption of the pumps in the solar thermal plant participates to the operating cost of the plant. The pumps are variable speed ones circulating the fluid in the different parts of the plant and are represented with the following equations:

$$\dot{P}_{hydrau} = \frac{\dot{m}_{max}}{\rho} \Delta P_{max} (\dot{m}_{max}) \quad (\text{A.10})$$

$$\dot{P}_{elec} = \frac{\dot{P}_{hydrau}}{\eta_{pump}} \left( \frac{\dot{m}}{\dot{m}_{max}} \right)^3 \quad (\text{A.11})$$

With:

$\dot{P}_{hydrau}$  maximum pumping power [ $W$ ],

$\dot{m}_{max}$  maximum flow rate allowed in the pump [ $kg.s^{-1}$ ],  
 $\Delta P_{max}$  pressure drop at the maximum flow rate [ $Pa$ ],  
 $\dot{P}_{elec}$  electric power [ $W$ ],  
 $\dot{m}$  actual flow rate [ $kg.s^{-1}$ ],  
 $\eta_{pump}$  overall efficiency of the pump.

The pumps are not described more precisely in the circuit, only their electric consumption is computed. The electric power should be minimized to reduce the operating costs but also the CO<sub>2</sub> emissions associated with heat production.

#### *Appendix A.6. Representation of the various operating modes*

The model for the complete solar thermal plant is obtained by connecting the models for the different elements of the plant: solar field, heat exchangers, storage tank, pumps and pipes. The solar thermal plant can be operated with several modes depending on the weather conditions, the storage level and the heat demand, and different equations are used for each mode. For example, the assumption of a linear variation of the temperature inside the solar field only stands when the solar field is in operation and a fluid is flowing through it (with a flow rate  $\dot{m}_{SF}$ ). Otherwise, another equation should be used, such as fixing the outlet temperature equal to the inlet temperature. Two conditional equations can be written as follows:

$$\left\{ \begin{array}{l} T_{SF}^{out} = T_{SF}^{in} \text{ if } \dot{m}_{SF} = 0 \\ \text{and} \\ T_{SF}^{out} = 2T_{SF}^{mean} - T_{SF}^{in} \text{ if } \dot{m}_{SF} \neq 0 \end{array} \right.$$

To represent these conditional equations in our optimization framework, sigmoid functions and Big M inequalities are used as follows:

$$sig(\dot{m}_{SF}) = \frac{1}{1 + exp^{-\beta(\dot{m}_{SF} - \delta)}} \quad (A.12)$$

With:

$\beta$  parameter characterizing the steepness of the sigmoid,

$\delta$  threshold for the variable  $\dot{m}_{SF}$ .

The sigmoid function represents the existence of a flow rate in the solar field or not. It replaces the binary variable typically used in Big M inequalities for mixed-integer problems [57] by a continuous function suitable for non linear programming problems. If the flow rate in the solar field is below the threshold  $\delta$ , the sigmoid function is zero and otherwise it is 1. To represent the existence of a flow rate, a small value of  $\delta$  is chosen. In the real system, a very small flow rate is not implementable by the pumps and valves. Thus, a value of  $1kg.s^{-1}$  was chosen to avoid that a very small flow rate impacts the solar thermal plant operation in a non realistic way.  $\beta$  needs to be adjusted to achieve the best compromise between a good reproduction of a binary variable behavior and an easy and fast convergence. The sigmoid is used in Big M inequalities as follows:

$$\left\{ \begin{array}{l} -sig(\dot{m}_{SF})M + T_{SF}^{in} \leq T_{SF}^{out} \leq sig(\dot{m}_{SF})M + T_{SF}^{in} \\ \text{and} \\ -(1 - sig(\dot{m}_{SF}))M + 2T_{SF}^{mean} - T_{SF}^{in} \leq T_{SF}^{out} \leq (1 - sig(\dot{m}_{SF}))M + 2T_{SF}^{mean} - T_{SF}^{in} \end{array} \right.$$

With M a scalar much larger than the variable considered. These two inequalities will hold for every  $\dot{m}_{SF}$  but the most limiting constraint will impose a value to  $T_{SF}^{out}$ .

Such a continuous formulation is useful to represent the various operating modes of the solar thermal plant such as the shut down of the solar circuit leading to no exchanged power in heat exchanger 1, or the interruption of supply of solar heat to the consumer through the heat exchanger 2 because there is no solar energy available directly from the solar field or from the storage tank.

## References

- [1] United Nations Framework Convention on Climate Change, Adoption of the paris agreement, 21st Conference of the Parties.

URL [https://unfccc.int/sites/default/files/english\\_paris\\_agreement.pdf](https://unfccc.int/sites/default/files/english_paris_agreement.pdf)

- [2] U. Collier, Renewable Heat Policies - Delivering clean heat solutions for the energy transition, Insights Series 2018 - International Energy Agency.  
URL [https://iea.blob.core.windows.net/assets/f5a7c5e2-f794-44ea-87bb-50fb07dd483a/Renewable\\_Heat\\_Policies.pdf](https://iea.blob.core.windows.net/assets/f5a7c5e2-f794-44ea-87bb-50fb07dd483a/Renewable_Heat_Policies.pdf)
- [3] Renewable Energy Directive, Directive (EU) 2018/2001 of the European Parliament and of the Council of 11 December 2018 on the promotion of the use of energy from renewable sources, OJ L328/82.  
URL <https://eur-lex.europa.eu/eli/dir/2018/2001/oj>
- [4] Y. Tian, C. Zhao, A review of solar collectors and thermal energy storage in solar thermal applications, Applied Energy 104 (2013) 538–553. doi:10.1016/j.apenergy.2012.11.051.
- [5] International Energy Agency, Requirements & guidelines for collector loop installation, Task 45, Solar Heating & Cooling Program.  
URL <http://task45.iea-shc.org/data/sites/1/publications/IEA-SHC-T45.A.2-TECH-Collector-loop-reqs.pdf>
- [6] B. Koçak, A. I. Fernandez, H. Paksoy, Review on sensible thermal energy storage for industrial solar applications and sustainability aspects, Solar Energy 209 (2020) 135–169. doi:10.1016/j.solener.2020.08.081.
- [7] W. Weiss, M. Spörk-Dür, Global Market Development and Trends in 2020 Detailed Market Data 2019, Solar Heating and Cooling Programme - International Energy Agency.  
URL <https://www.iea-shc.org/Data/Sites/1/publications/Solar-Heat-Worldwide-2021.pdf>
- [8] E. Lygouras, A. G. Papatsounis, P. N. Botsaris, A. Pechtelidis, Optimization & techno-economic analysis of a hybrid system with thermal energy storage within a LEC, Renewable Energy 215 (2023) 118920. doi:10.1016/j.renene.2023.118920.

- [9] T. Yang, W. Liu, Q. Sun, W. Hu, G. J. Kramer, Techno-economic-environmental analysis of seasonal thermal energy storage with solar heating for residential heating in China, *Energy* 283 (2023) 128389. doi:10.1016/j.energy.2023.128389.
- [10] R. Zhang, D. Wang, Z. Yu, Y. Sun, H. Wan, Y. Liu, Q. Jiao, M. Gao, J. Fan, B. Lan, Dual-objective optimization of large-scale solar heating systems integrated with water-to-water heat pumps for improved techno-economic performance, *Energy and Buildings* 296 (2023) 113281. doi:10.1016/j.enbuild.2023.113281.
- [11] A. Rahbari, A. Fontalvo, J. Pye, Solar-thermal beneficiation of iron ore: System-level dynamic simulation and techno-economic optimisation, *Applied Thermal Engineering* 223 (2023) 119794. doi:10.1016/j.applthermaleng.2022.119794.
- [12] F. B. Tilahun, R. Bhandari, M. Mamo, Design optimization of a hybrid solar-biomass plant to sustainably supply energy to industry: Methodology and case study, *Energy* 220 (2021) 119736. doi:10.1016/j.energy.2020.119736.
- [13] M. Krause, K. Vajen, F. Wiese, H. Ackermann, Investigations on optimizing large solar thermal systems, *Solar Energy* 73 (2003) 217–225. doi:10.1016/S0038-092X(02)00111-1.
- [14] E. Camacho, F. Rubio, M. Berenguel, L. Valenzuela, A survey on control schemes for distributed solar collector fields. Part I: Modeling and basic control approaches, *Solar Energy* 81 (10) (2007) 1240–1251. doi:10.1016/j.solener.2007.01.002.
- [15] M. L. Darby, M. Nikolaou, J. Jones, D. Nicholson, RTO: An overview and assessment of current practice, *Journal of Process Control* 21 (2011) 874–884. doi:10.1016/j.jprocont.2011.03.009.

- [16] E. Camacho, F. Rubio, M. Berenguel, L. Valenzuela, A survey on control schemes for distributed solar collector fields. Part II: Advanced control approaches, *Solar Energy* 81 (10) (2007) 1252–1272. doi:10.1016/j.solener.2007.01.001.
- [17] A. O. López-Bautista, A. Flores-Tlacuahuac, M. A. Gutiérrez-Limón, Robust model predictive control for a nanofluid based solar thermal power plant, *Journal of Process Control* 94 (2020) 97–109. doi:10.1016/j.jprocont.2020.09.001.
- [18] G. Csordas, A. Brunger, K. Hollands, M. Lightstone, Plume entrainment effects in solar domestic hot water systems employing variable-flow-rate control strategies, *Solar Energy* 49 (6) (1992) 497–505. doi:10.1016/0038-092X(92)90158-7.
- [19] S. Engell, Feedback control for optimal process operation, *Journal of Process Control* 17 (2007) 203–219. doi:10.1016/j.jprocont.2006.10.011.
- [20] S. Pintaldi, J. Li, S. Sethuvenkatraman, S. White, G. Rosengarten, Model predictive control of a high efficiency solar thermal cooling system with thermal storage, *Energy and Buildings* 196 (2019) 214–226. doi:10.1016/j.enbuild.2019.05.008.
- [21] G. Serale, M. Fiorentini, A. Capozzoli, P. Cooper, M. Perino, Formulation of a model predictive control algorithm to enhance the performance of a latent heat solar thermal system, *Energy Conversion and Management* 173 (2018) 438–449. doi:10.1016/j.enconman.2018.07.099.
- [22] A. Caspari, C. Tsay, A. Mhamdi, M. Baldea, A. Mitsos, The integration of scheduling and control: Top-down vs. bottom-up, *Journal of Process Control* 91 (2020) 50–62. doi:10.1016/j.jprocont.2020.05.008.
- [23] S. Scolan, S. Serra, S. Sochard, P. Delmas, J.-M. Reneaume, Dynamic optimization of the operation of a solar thermal plant, *Solar Energy* 198 (2020) 643–657. doi:10.1016/j.solener.2020.01.076.

- [24] R. Delubac, S. Serra, S. Sochard, J.-M. Reneaume, A Dynamic Optimization Tool to Size and Operate Solar Thermal District Heating Networks Production Plants, *Energies* 14 (23) (2021) 8003. doi:10.3390/en14238003.
- [25] J. Immonen, K. M. Powell, Dynamic optimization with flexible heat integration of a solar parabolic trough collector plant with thermal energy storage used for industrial process heat, *Energy Conversion and Management* 267 (2022) 115921. doi:10.1016/j.enconman.2022.115921.
- [26] M. J. Wagner, W. T. Hamilton, A. Newman, J. Dent, C. Diep, R. Braun, Optimizing dispatch for a concentrated solar power tower, *Solar Energy* 174 (2018) 1198–1211. doi:10.1016/j.solener.2018.06.093.
- [27] M. Wittmann, M. Eck, R. Pitz-Paal, H. Müller-Steinhagen, Methodology for optimized operation strategies of solar thermal power plants with integrated heat storage, *Solar Energy* 85 (2011) 653–659. doi:10.1016/j.solener.2010.11.024.
- [28] K. M. Powell, J. D. Hedengren, T. F. Edgar, Dynamic optimization of a hybrid solar thermal and fossil fuel system, *Solar Energy* 108 (2014) 210–218. doi:10.1016/j.solener.2014.07.004.
- [29] P. G. Brodrick, A. R. Brandt, L. J. Durlofsky, Optimal design and operation of integrated solar combined cycles under emissions intensity constraints, *Applied Energy* 226 (2018) 979–990. doi:10.1016/j.apenergy.2018.06.052.
- [30] K. Ellingwood, K. Mohammadi, K. Powell, Dynamic optimization and economic evaluation of flexible heat integration in a hybrid concentrated solar power plant, *Applied Energy* 276 (2020) 115513. doi:10.1016/j.apenergy.2020.115513.
- [31] X. Li, T. Li, L. Liu, Z. Wang, X. Li, J. Huang, J. Huang, P. Guo, W. Xiong, Operation optimization for integrated energy system based on

- hybrid CSP-CHP considering power-to-gas technology and carbon capture system, *Journal of Cleaner Production* 391 (2023) 136119. doi:10.1016/j.jclepro.2023.136119.
- [32] J. V. Kadam, M. Schlegel, W. Marquardt, R. L. Tousain, D. H. Van Hessem, J. Van Den Berg, O. H. Bosgra, A Two-Level Strategy of Integrated Dynamic Optimization and Control of Industrial Processes - a Case Study, in: *European Symposium on Computer Aided Process Engineering*, Vol. 12, Elsevier, The Hague, The Netherlands, 2002, pp. 511–516. doi:10.1016/S1570-7946(02)80113-4.
- [33] P. Joy, E. S. Schultz, F. Ebrahimi, U. Turan, S. Casteel, T. Schaffrath, R. Hammen, A. Mhamdi, Dynamic optimization and nonlinear model predictive control of a semi-batch epoxidation process, *Journal of Process Control* 108 (2021) 55–67. doi:10.1016/j.jprocont.2021.10.013.
- [34] D. Elixmann, J. Busch, W. Marquardt, Integration of model-predictive scheduling, dynamic real-time optimization and output tracking for a wastewater treatment process, in: *IFAC Proceedings Volumes - 11th International Symposium on Computer Applications in Biotechnology*, Vol. 43, Elsevier, Leuven, Belgium, 2010, pp. 90–95. doi:10.3182/20100707-3-BE-2012.0042.
- [35] V. De Oliveira, J. Jaschke, S. Skogestad, Dynamic online optimization of a house heating system in a fluctuating energy price scenario, in: *IFAC Proceedings Volumes - 10th International Symposium on Dynamics and Control of Process Systems*, Elsevier, Mumbai, India, 2013, pp. 463–468. URL <https://folk.ntnu.no/jaschke/preprints/2013/DeOliveiraHouseHeating/0070.pdf>
- [36] I. M. L. Pataro, L. Roca, J. L. G. Sanches, M. Berenguel, An economic D-RTO for thermal solar plant: analysis and simulations based on a feedback linearization control case, in: *XXIII Congresso Brasileiro de Automática*, Virtual event, 2020. doi:10.48011/asba.v2i1.1294.

URL [https://sba.org.br/open\\_journal\\_systems/index.php/cba/article/view/1294](https://sba.org.br/open_journal_systems/index.php/cba/article/view/1294)

- [37] E. Saloux, J. A. Candanedo, Model-based predictive control to minimize primary energy use in a solar district heating system with seasonal thermal energy storage, *Applied Energy* 291 (2021) 116840. doi:10.1016/j.apenergy.2021.116840.
- [38] A. Untrau, S. Sochard, F. Marias, J.-M. Reneaume, G. A. C. Le Roux, S. Serra, Dynamic Real-Time Optimization of a solar thermal plant during daytime, *Computers & Chemical Engineering* 172 (2023) 108184. doi:10.1016/j.compchemeng.2023.108184.
- [39] A. Untrau, S. Sochard, F. Marias, J.-M. Reneaume, G. A. Le Roux, S. Serra, Analysis and future perspectives for the application of Dynamic Real-Time Optimization to solar thermal plants: A review, *Solar Energy* 241 (2022) 275–291. doi:10.1016/j.solener.2022.05.058.
- [40] International Energy Agency, Integration guideline, solar process heat for production and advanced applications, Task 49, Solar Heating & Cooling Program.  
URL [https://task49.iea-shc.org/Data/Sites/1/publications/150218\\_IEA%20Task%2049\\_D\\_B2\\_Integration\\_Guideline-final1.pdf](https://task49.iea-shc.org/Data/Sites/1/publications/150218_IEA%20Task%2049_D_B2_Integration_Guideline-final1.pdf)
- [41] A. Untrau, S. Sochard, F. Marias, J.-M. Reneaume, G. A. C. Le Roux, S. Serra, A fast and accurate 1-dimensional model for dynamic simulation and optimization of a stratified thermal energy storage, *Applied Energy* 333 (2023) 120614. doi:10.1016/j.apenergy.2022.120614.
- [42] J. Huang, J. Fan, S. Furbo, Feasibility study on solar district heating in China, *Renewable and Sustainable Energy Reviews* 108 (2019) 53–64. doi:10.1016/j.rser.2019.03.014.
- [43] I. Petkov, P. Gabrielli, Power-to-hydrogen as seasonal energy storage: an uncertainty analysis for optimal design of low-carbon multi-energy sys-

- tems, *Applied Energy* 274 (2020) 115197. doi:10.1016/j.apenergy.2020.115197.
- [44] J. D. Hedengren, R. A. Shishavan, K. M. Powell, T. F. Edgar, Nonlinear modeling, estimation and predictive control in APMonitor, *Computers & Chemical Engineering* 70 (2014) 133–148. doi:10.1016/j.compchemeng.2014.04.013.
- [45] A. DON MAHAWATTEGE, Prix du gaz naturel en France et dans l’Union européenne en 2020, Commissariat général au développement durable.  
URL [https://www.statistiques.developpement-durable.gouv.fr/sites/default/files/2021-05/datalab\\_essentiel\\_246\\_prix\\_gaz\\_naturel\\_2020\\_juin2021.pdf](https://www.statistiques.developpement-durable.gouv.fr/sites/default/files/2021-05/datalab_essentiel_246_prix_gaz_naturel_2020_juin2021.pdf)
- [46] A. DON MAHAWATTEGE, Prix de l’électricité en France et dans l’Union européenne en 2020, Commissariat général au développement durable.  
URL [https://www.statistiques.developpement-durable.gouv.fr/sites/default/files/2021-06/datalab\\_essentiel\\_248\\_prix\\_de\\_l\\_electricite\\_en\\_france\\_et\\_dans\\_l\\_union\\_europeenne\\_en\\_2020\\_juin2021.pdf](https://www.statistiques.developpement-durable.gouv.fr/sites/default/files/2021-06/datalab_essentiel_248_prix_de_l_electricite_en_france_et_dans_l_union_europeenne_en_2020_juin2021.pdf)
- [47] G. Kahvecioğlu, D. P. Morton, M. J. Wagner, Dispatch optimization of a concentrating solar power system under uncertain solar irradiance and energy prices, *Applied Energy* 326 (2022) 119978. doi:10.1016/j.apenergy.2022.119978.
- [48] S. Scolan, Développement d’un outil de simulation et d’optimisation dynamique d’une centrale solaire thermique., thesis, Pau (Jul. 2020).  
URL <https://www.theses.fr/2020PAUU3007>
- [49] ISO/FDIS 9806, Énergie solaire - capteurs thermiques solaires - méthodes d’essai, International Standard.  
URL <https://www.iso.org/fr/standard/67978.html>

- [50] L. Wang, B. Sundén, M. Manglik, Plate Heat Exchangers: Design, Applications and Performance, WIT Press, 2007, iISBN: 978-1853127373.
- [51] K. M. Powell, T. F. Edgar, An adaptive-grid model for dynamic simulation of thermocline thermal energy storage systems, *Energy Conversion and Management* 76 (2013) 865–873. doi:10.1016/j.enconman.2013.08.043.
- [52] G. Carey, B. A. Finlayson, Orthogonal collocation on finite elements, *Chemical Engineering Science* 30 (5-6) (1975) 587–596. doi:10.1016/0009-2509(75)80031-5.
- [53] R. A. Pate, A Thermal Energy Storage Tank Model for Solar Heating, thesis, Utah State University (1977). doi:10.26076/2a5d-3188.
- [54] R. De Césaro Oliveski, A. Krenzinger, H. A. Vielmo, Comparison between models for the simulation of hot water storage tanks, *Solar Energy* 75 (2) (2003) 121–134. doi:10.1016/j.solener.2003.07.009.
- [55] R. Franke, Object-oriented modeling of solar heating systems, *Solar Energy* 60 (1997) 171–180. doi:10.1016/S0038-092X(96)00156-9.
- [56] E. Kleinbach, W. Beckman, S. Klein, Performance study of one-dimensional models for stratified thermal storage tanks, *Solar Energy* 50 (2) (1993) 155–166. doi:10.1016/0038-092X(93)90087-5.
- [57] F. Glover, Improved linear integer programming formulations of nonlinear integer problems, *Management Science* 22 (4) (1975) 455–460.  
URL <https://www.jstor.org/stable/2630109>